Supplementary Materials for
Charting spatial ligand-target activity using Renoir

Narein Rao[1], Tanush Kumar[2], Rhea Pai[3,4], Archita Mishra[5,6], Florent Ginhoux[7,8], Jerry Chan[6], Ankur Sharma[3,4,6,9,10,*], and Hamim Zafar[1,11,12,*]

[1]Department of Computer Science and Engineering, Indian Institute of Technology Kanpur, India
[2]Department of Mathematics and Statistics, Indian Institute of Technology Kanpur, India
[3]Harry Perkins Institute of Medical Research, Nedlands, Perth, Western Australia
[4]Curtin Medical School, Curtin University, Perth, Western Australia
[5]University of Sydney, Sydney, Australia
[6]KK Research Center, KK Women's and Children's Hospital, Singapore
[7]Singapore Immunology Network (SIgN), Agency for Science, Technology and Research (ASTAR), Singapore
[8]Gustave Roussy Cancer Campus, Villejuif, France
[9]Translational Genomics Program, Garvan Institute of Medical Research, Darlinghurst, Australia
[10]School of Clinical Medicine, Faculty of Medicine and Health, University of New South Wales, Kensington, Australia
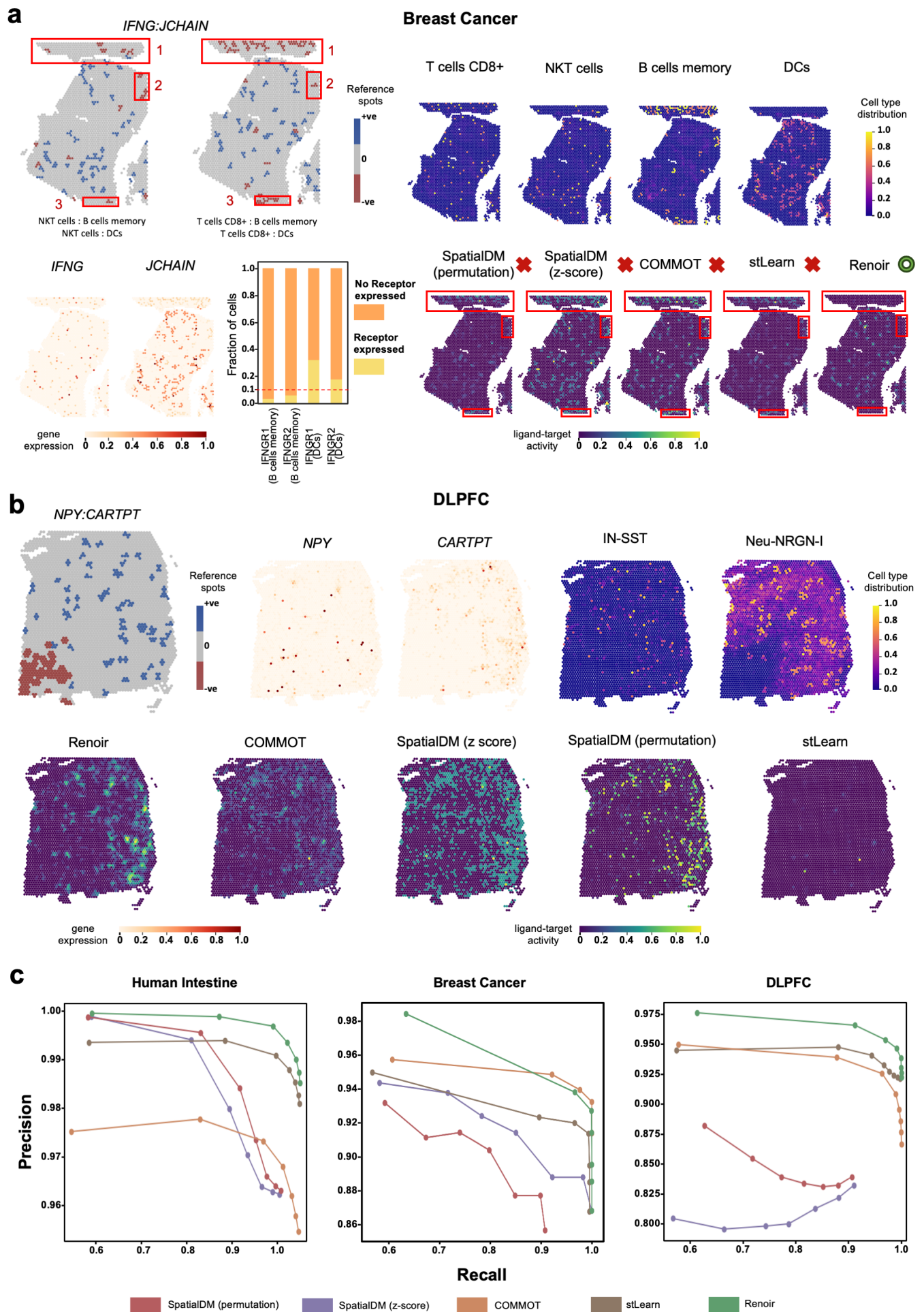[11]Department of Biological Sciences and Bioengineering, Indian Institute of Technology Kanpur, India
[12]Mehta Family Center for Engineering in Medicine, Indian Institute of Technology Kanpur, India
*Corresponding Author
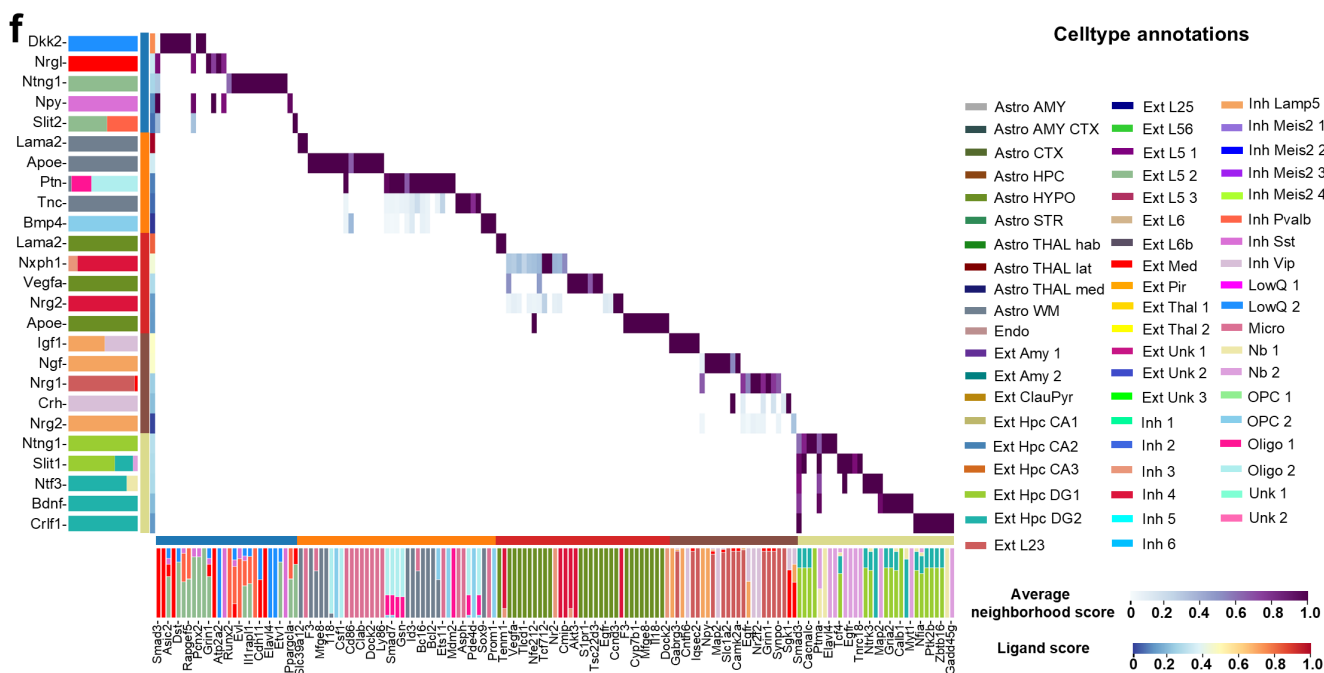[3,4,6,9,10]ankur.sharma@garvan.org.au (A.S.), [1,11,12]hamim@iitk.ac.in (H.Z.)

Supplementary Figures

a

IFNG:JCHAIN

NKT cells : B cells memory
NKT cells : DCs

T cells CD8+ : B cells memory
T cells CD8+ : DCs

Reference spots
+ve
0
-ve

Breast Cancer

T cells CD8+ | NKT cells | B cells memory | DCs

Cell type distribution
1.0
0.8
0.6
0.4
0.2
0.0

IFNG | *JCHAIN*

gene expression 0 0.2 0.4 0.6 0.8 1.0

Fraction of cells

No Receptor expressed

Receptor expressed

IFNGR1 (B cells memory)
IFNGR2 (B cells memory)
IFNGR1 (DCs)
IFNGR2 (DCs)

SpatialDM (permutation) ✖ | SpatialDM (z-score) ✖ | COMMOT ✖ | stLearn ✖ | Renoir ◎

ligand-target activity 0 0.2 0.4 0.6 0.8 1.0

b

NPY:CARTPT

Reference spots
+ve
0
-ve

DLPFC

NPY | *CARTPT* | IN-SST | Neu-NRGN-I

Cell type distribution
1.0
0.8
0.6
0.4
0.2
0.0

Renoir | COMMOT | SpatialDM (z score) | SpatialDM (permutation) | stLearn

gene expression 0 0.2 0.4 0.6 0.8 1.0

ligand-target activity 0 0.2 0.4 0.6 0.8 1.0

c

Human Intestine | Breast Cancer | DLPFC

Precision

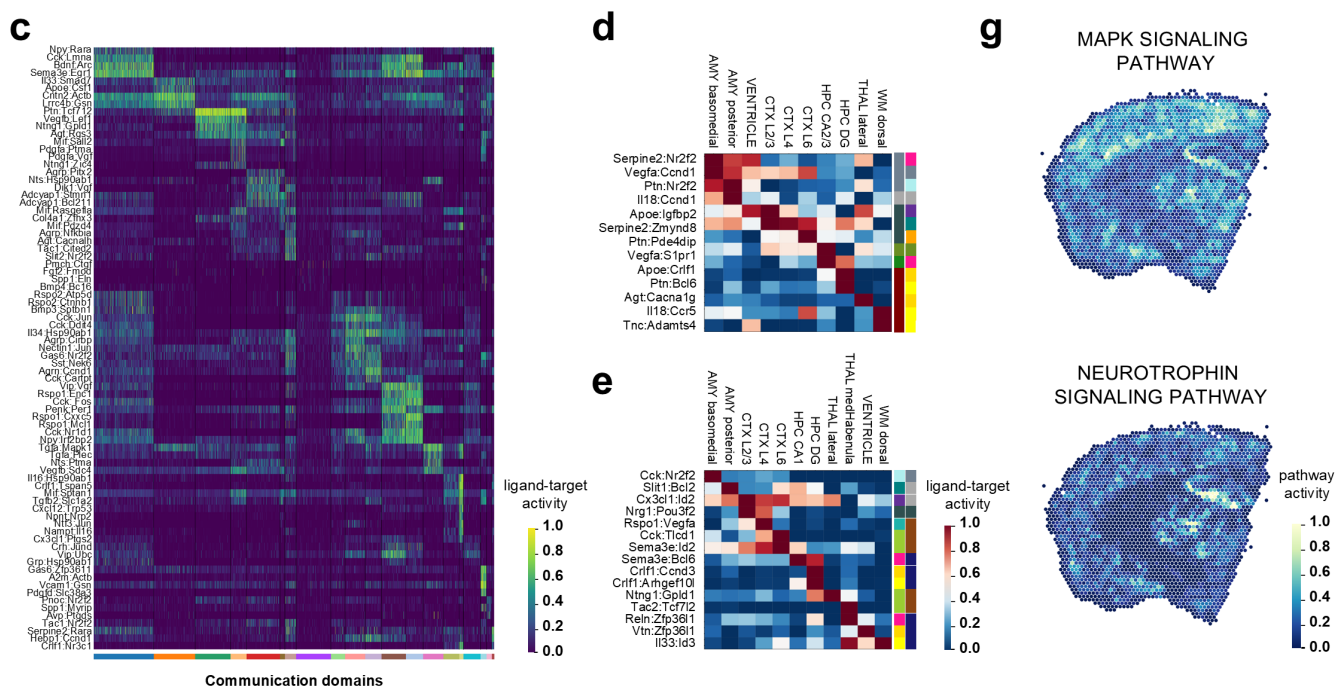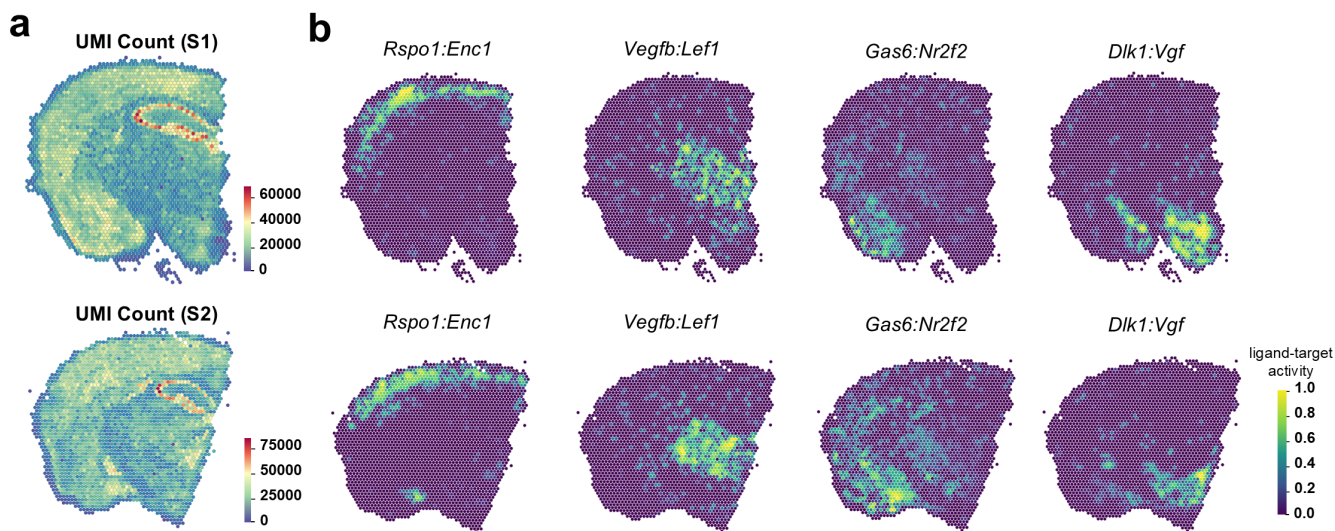Recall

SpatialDM (permutation) | SpatialDM (z-score) | COMMOT | stLearn | Renoir

Supplementary Figure 1: (a) Comparison of Renoir, SpatialDM, COMMOT, and stLearn for the simulated dataset for the ligand-target pair *IFNG-JCHAIN* simulated based on the TNBC dataset. Regions 1, 2 and 3 contain ligand and target expression, however, these regions harbor B memory cells which do not express the receptor for *IFNG* (*IFNGR1* and *IFNGR2*) making it unfeasible for these regions to harbor *IFNG-JCHAIN* activity. (b) Comparison of Renoir, SpatialDM, COMMOT, and stLearn for the simulated dataset for the ligand-target pair *NPY-CARTPT* simulated based on the DLPFC dataset (c) Comparison of Renoir, SpatialDM, COMMOT, and stLearn in terms of average precision and recall over all the ligand-target pairs across the tissue types across different threshold values used for calculating precision and recall. For varying threshold values, Renoir was able to consistently maintain high precision and recall values across the tissue types.
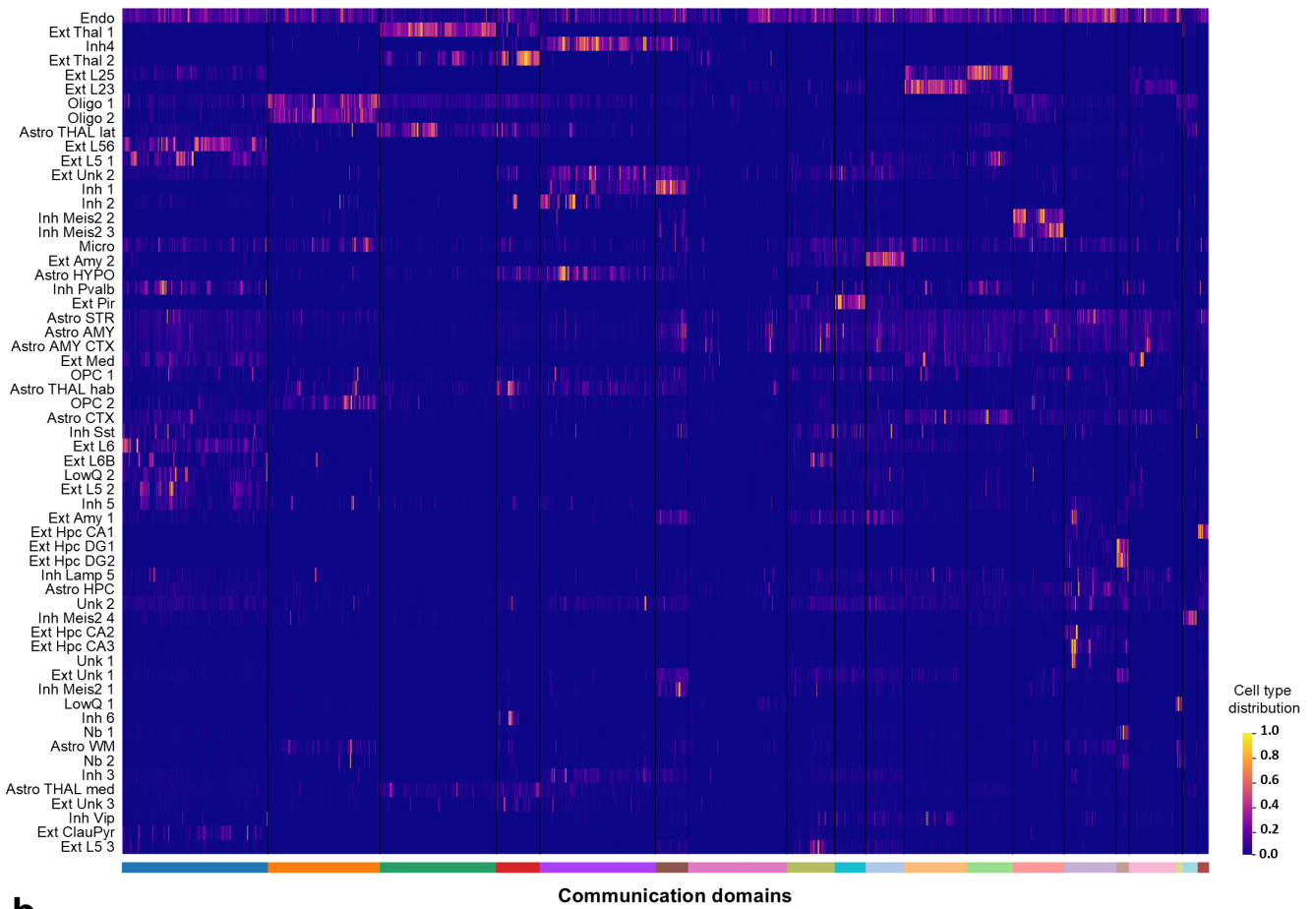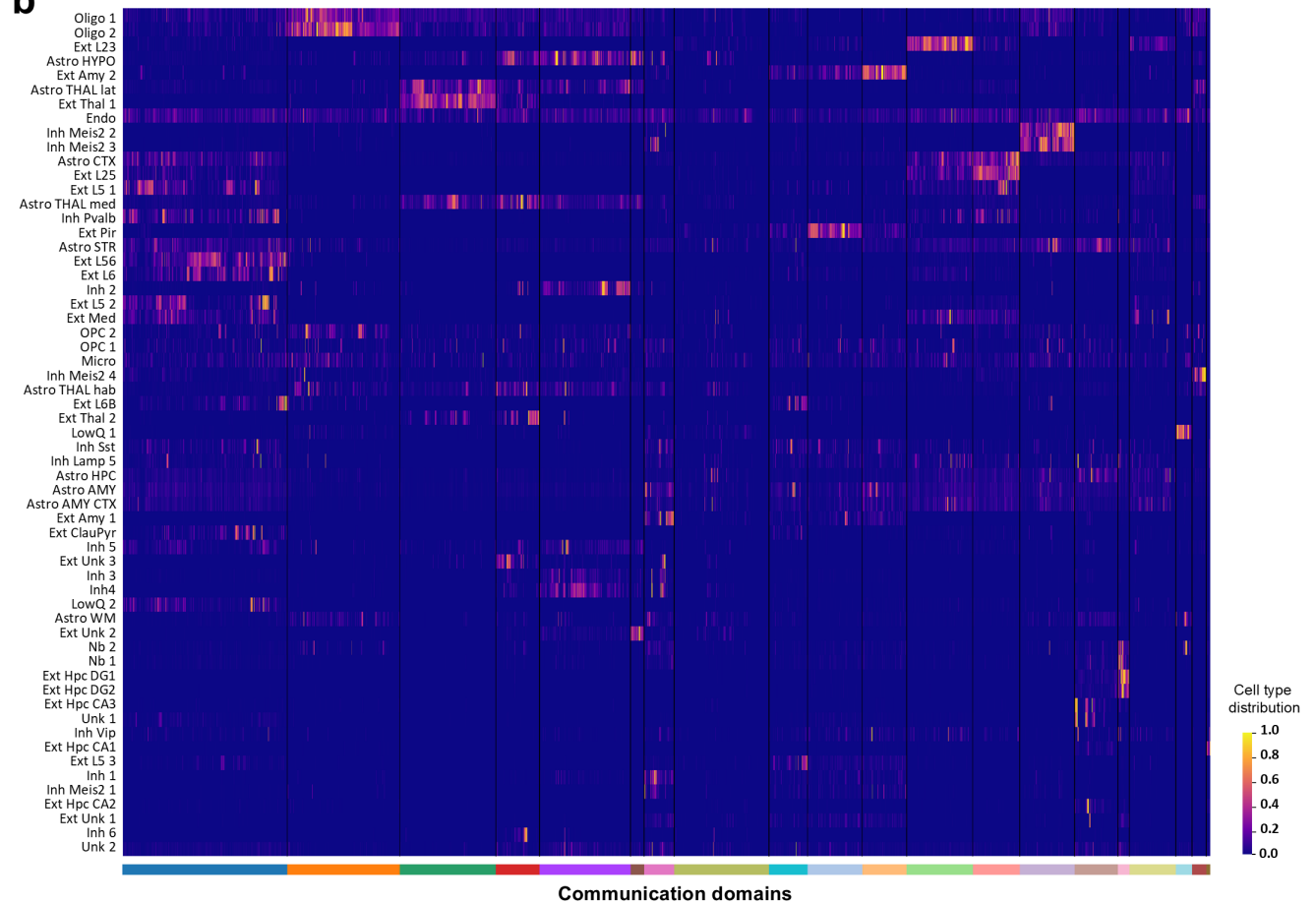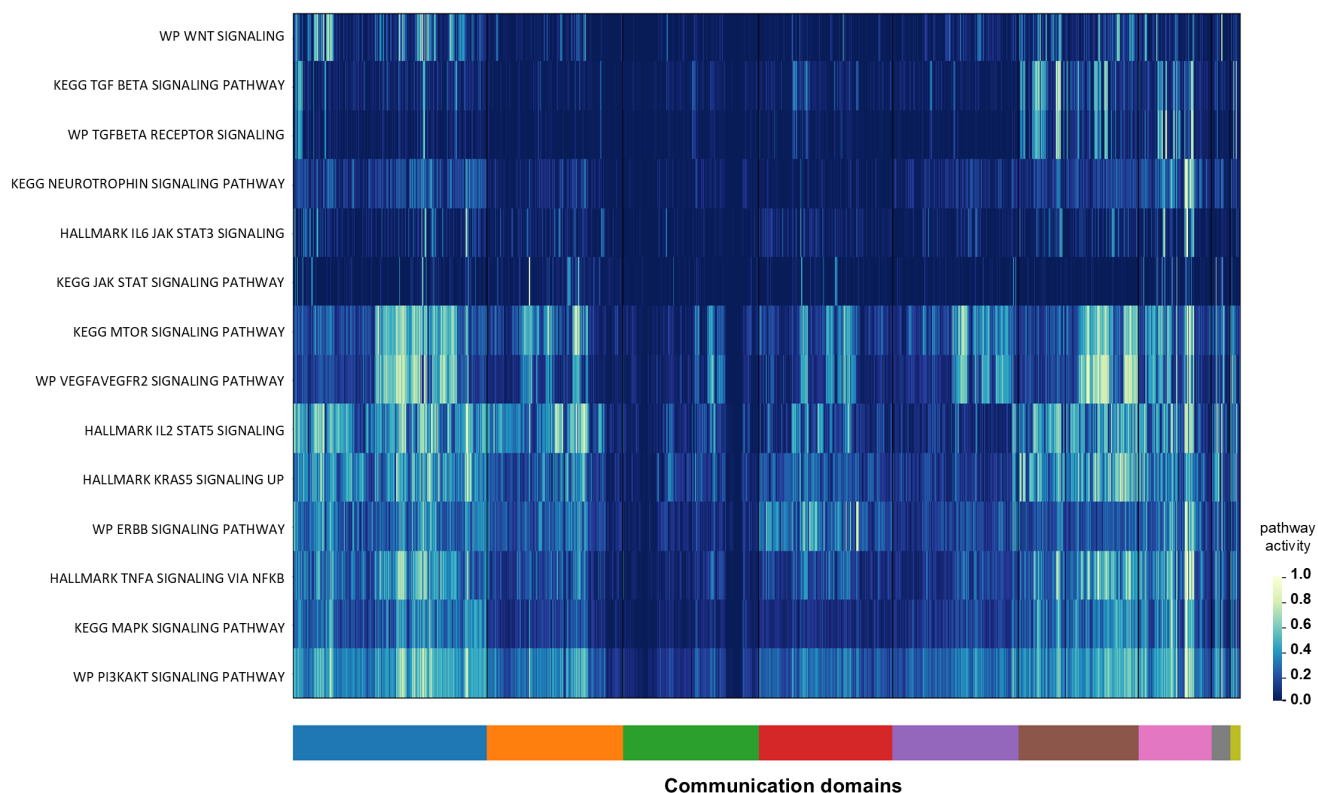
Supplementary Figure 2: Distribution of cell type abundances across the spots in mouse brain samples (a) S1 and (b) S2. The spots are ordered according to the spatial communication domains inferred by Renoir.

a UMI Count (S1)

UMI Count (S2)

b *Rspo1:Enc1* *Vegfb:Lef1* *Gas6:Nr2f2* *Dlk1:Vgf*

Rspo1:Enc1 *Vegfb:Lef1* *Gas6:Nr2f2* *Dlk1:Vgf*

ligand-target activity

c Communication domains

ligand-target activity

d

ligand-target activity

e

ligand-target activity

g MAPK SIGNALING PATHWAY

NEUROTROPHIN SIGNALING PATHWAY

pathway activity

f Celltype annotations

Astro AMY	Ext L25	Inh Lamp5
Astro AMY CTX	Ext L56	Inh Meis2 1
Astro CTX	Ext L5 1	Inh Meis2 2
Astro HPC	Ext L5 2	Inh Meis2 3
Astro HYPO	Ext L5 3	Inh Meis2 4
Astro STR	Ext L6	Inh Pvalb
Astro THAL hab	Ext L6b	Inh Sst
Astro THAL lat	Ext Med	Inh Vip
Astro THAL med	Ext Pir	LowQ 1
Astro WM	Ext Thal 1	LowQ 2
Endo	Ext Thal 2	Micro
Ext Amy 1	Ext Unk 1	Nb 1
Ext Amy 2	Ext Unk 2	Nb 2
Ext ClauPyr	Ext Unk 3	OPC 1
Ext Hpc CA1	Inh 1	OPC 2
Ext Hpc CA2	Inh 2	Oligo 1
Ext Hpc CA3	Inh 3	Oligo 2
Ext Hpc DG1	Inh 4	Unk 1
Ext Hpc DG2	Inh 5	Unk 2
Ext L23	Inh 6	

Average neighborhood score

Ligand score

Supplementary Figure 3: (a) Distribution of UMI count across mouse brain samples S1 and S2. (b) Spatial map of neighborhood activity scores for the ligand-target pairs across samples S1 and S2. (c) Differentially active ligand-target pairs inferred by Renoir across all communication domains for sample S2. (d) - (e) Characterization of ligand-target interactions between regional astrocyte subtypes and other co-localized cell types in sample S2. (d) Ligands expressed by regional astrocyte subtypes activating target genes in other cell types. (e) Target genes in regional astrocyte subtypes activated by ligands expressed by other co-localized cell types. (f) Communication domain-specific ranking of ligands based on cumulative activities over target genes expressed by major cell types in the domain for mouse brain sample S2. Top three ligands for each of eight communication domains are represented. Stacked color bars represent the cell types that express the ligand (right) and target (top). (g) Spatial map of MAPK SIGNALING and NEUROTROPHIN SIGNALING pathway activity across the spots in sample S2.
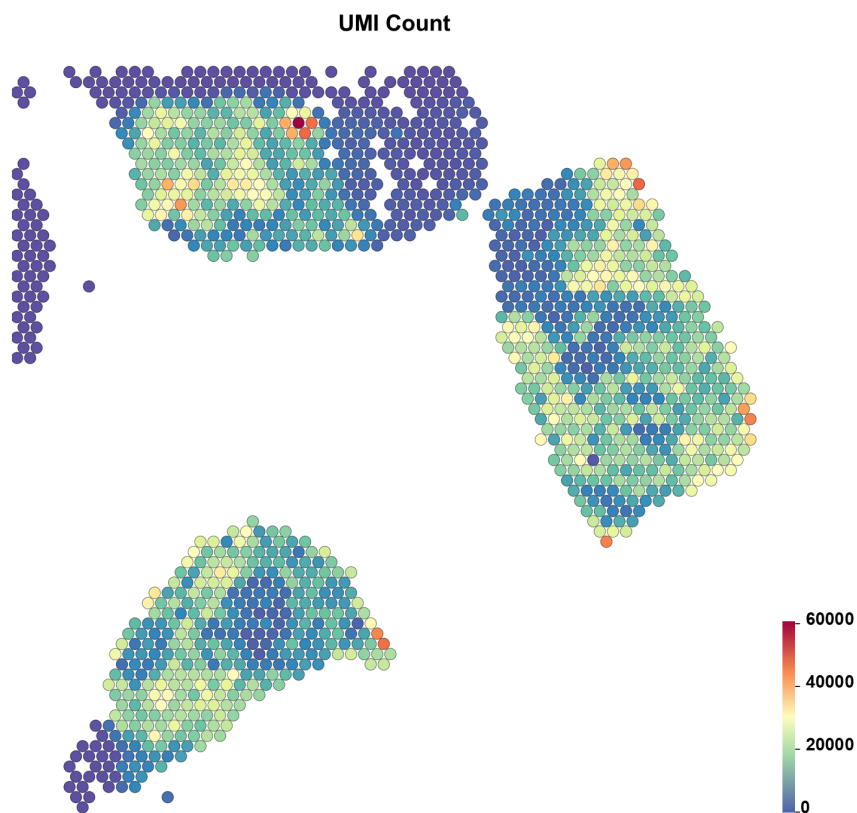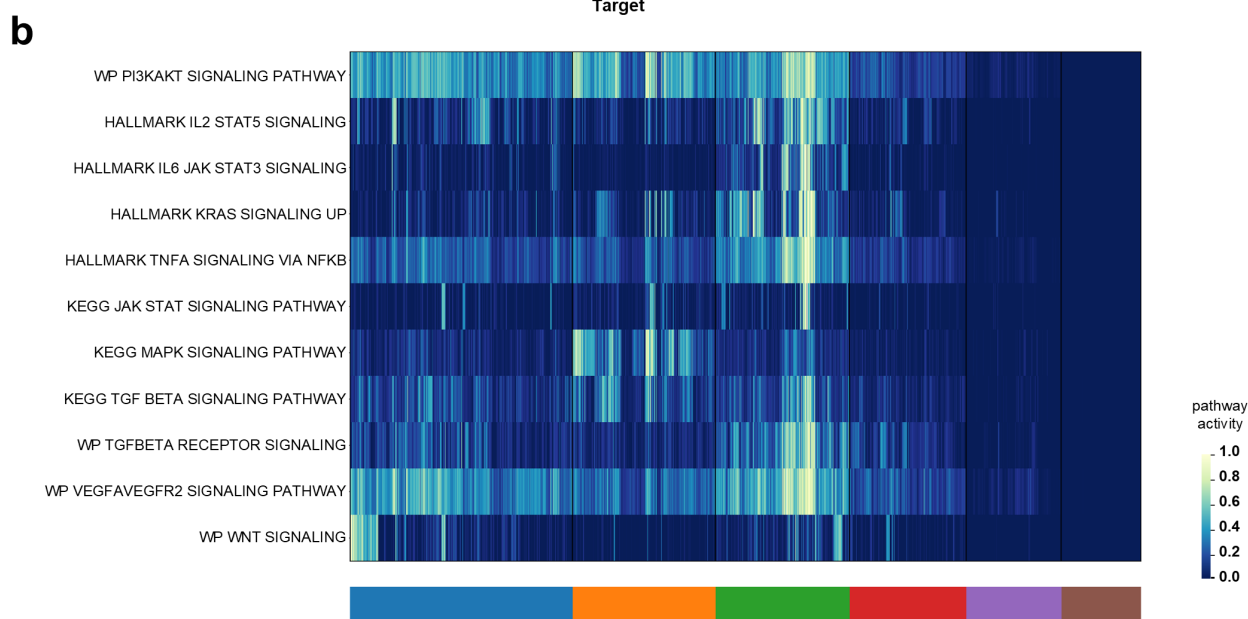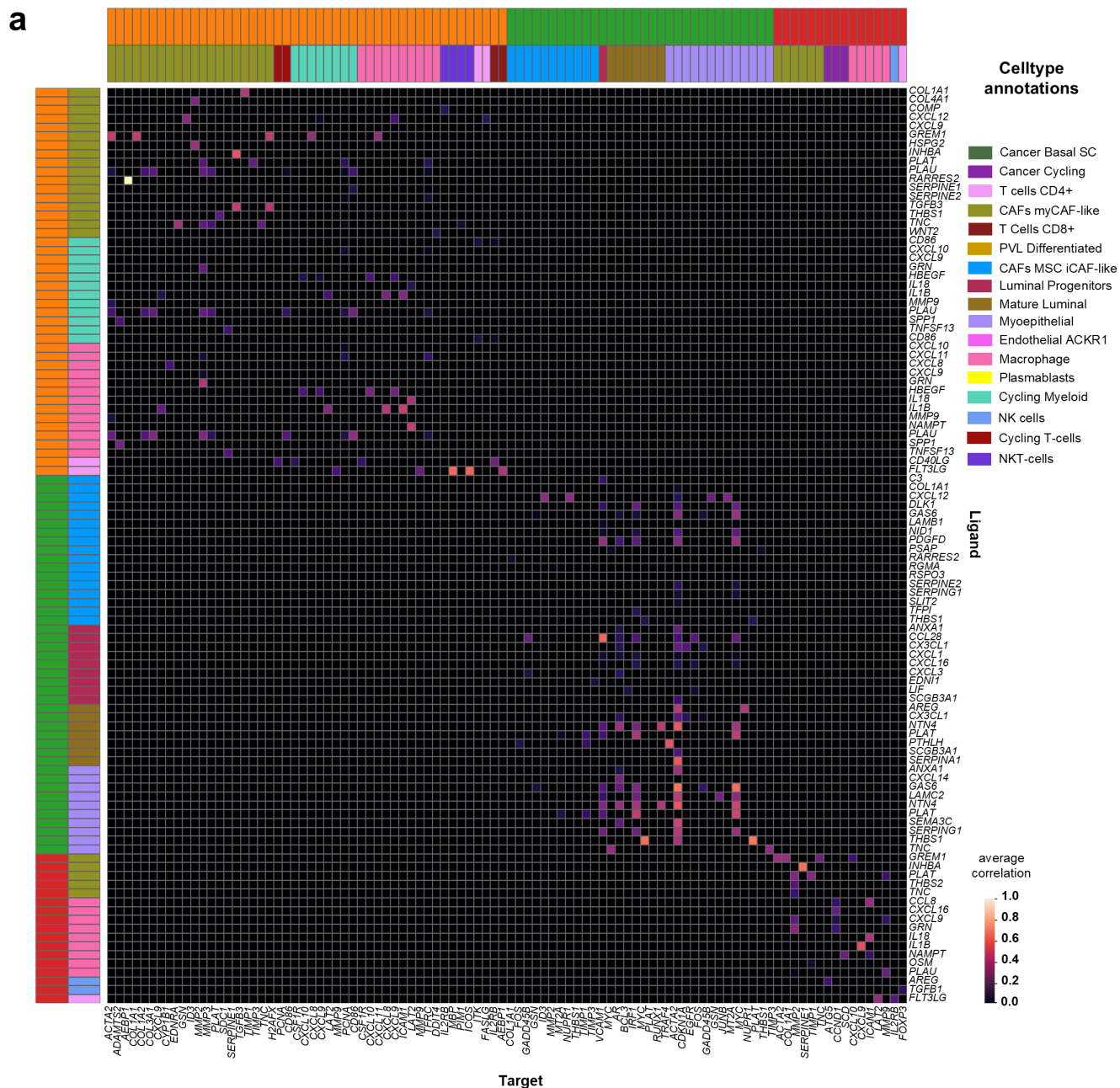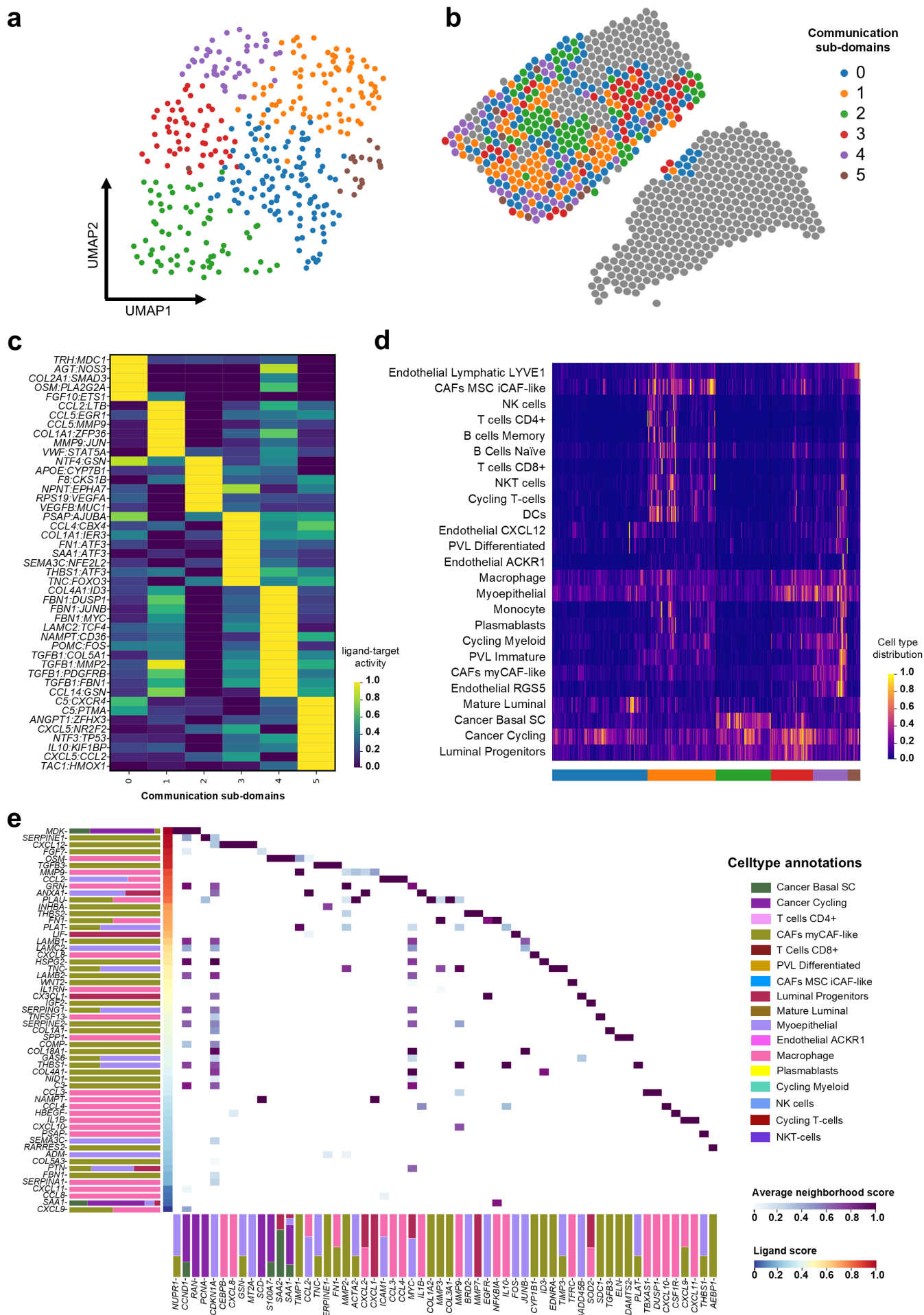
a

b
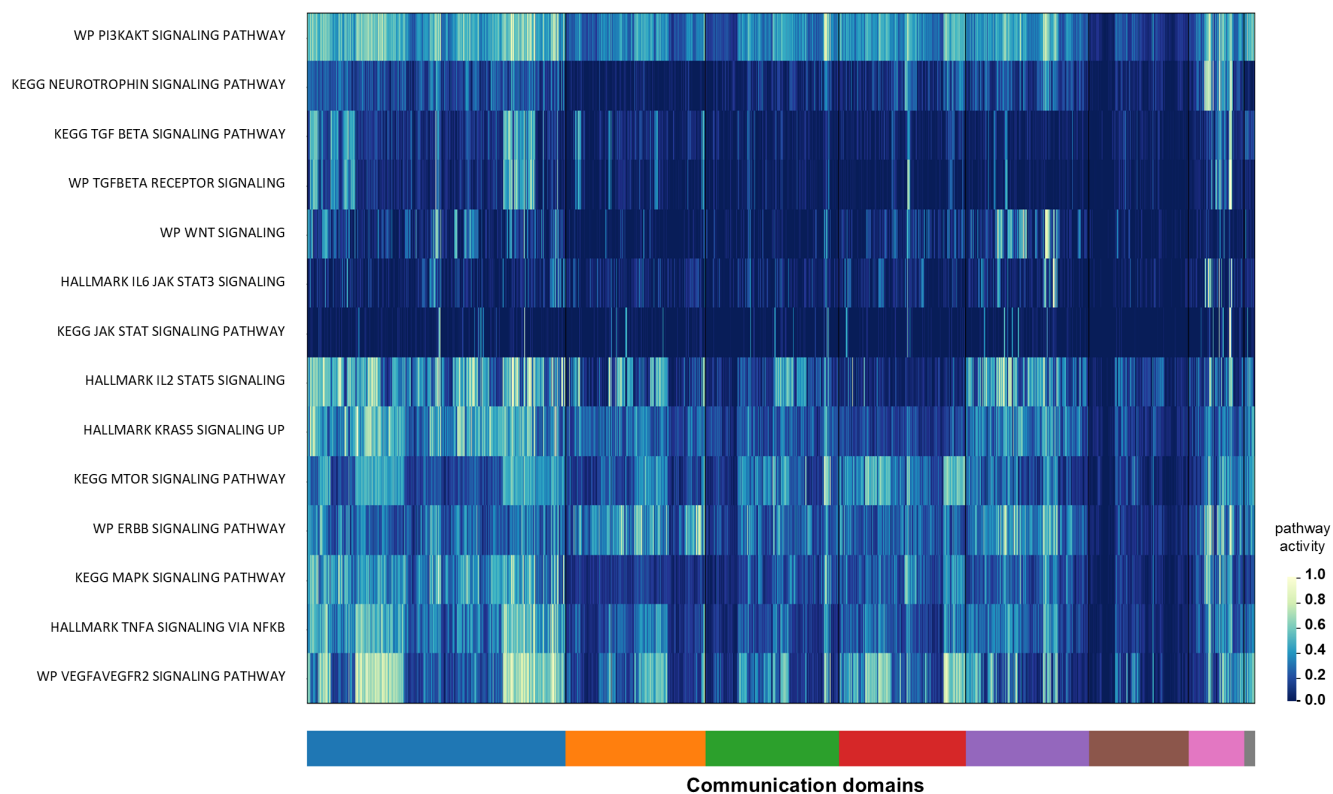
Supplementary Figure 4: (a) - (b) Distribution of various pathway activity across the spots in mouse brain samples (a) S1 and (b) S2. The spots are ordered according to the spatial communication domains inferred by Renoir.

a

b
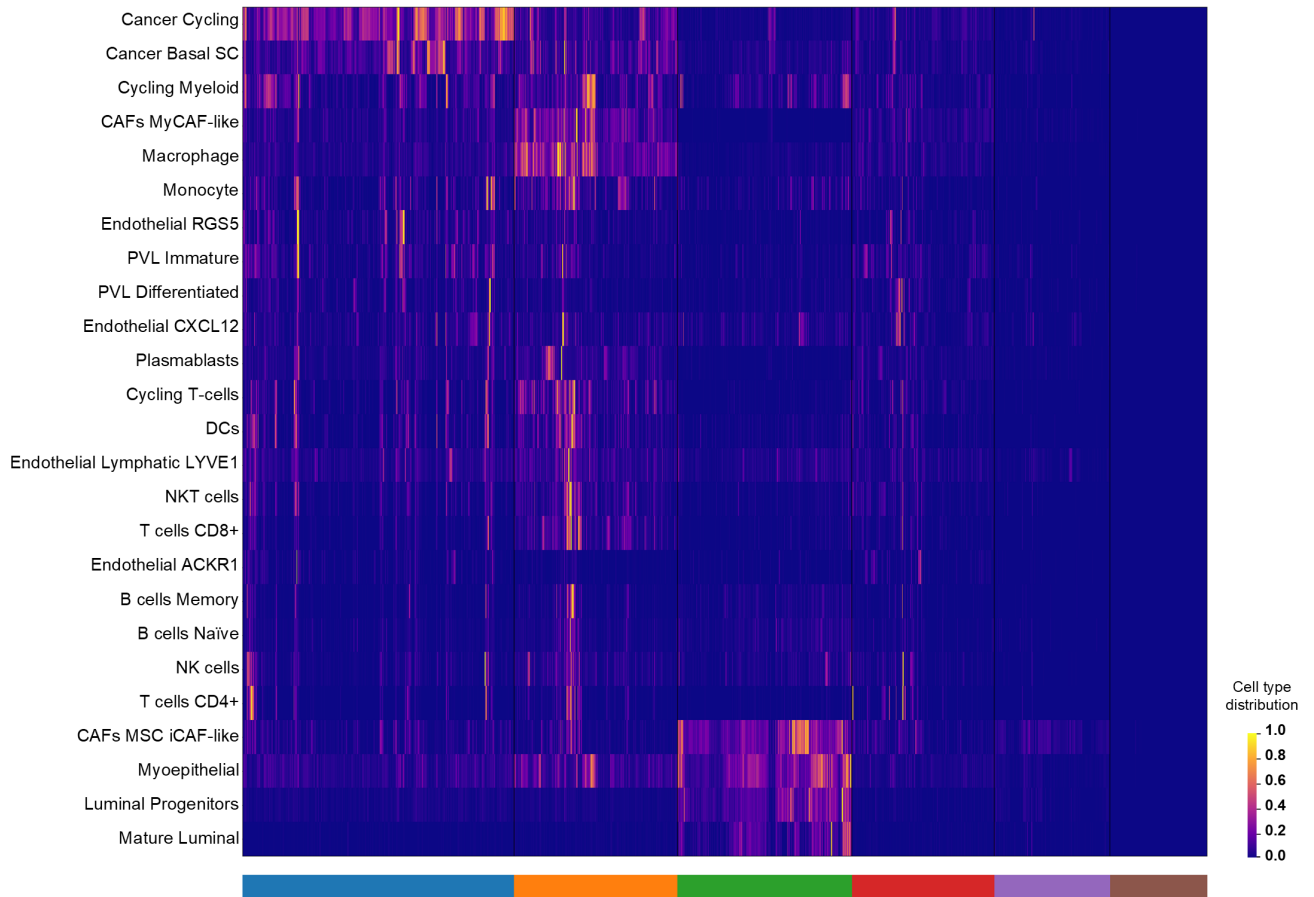
UMI Count

Supplementary Figure 5: (a) Distribution of cell types across spots in TNBC sample (b) Distribution of UMI count across the TNBC sample.

Supplementary Figure 6: (a) Cell type-specific ligand-target interactions inferred by Renoir for the TNBC dataset for the major cell types in domains 1, 2, and 3. The inner color bar represents the cell types of the ligand (left) and target (top) and the outer color bar represents the communication domain. Each cell represents the average Pearson correlation between the ligand-target neighborhood scores and the abundances of the cell types expressing the ligand and target across the spots pertaining to the domain being considered. (b) Distribution of pathway activities across the communication domains in the TNBC sample.

a

UMAP2

UMAP1

b

Communication sub-domains

- 0
- 1
- 2
- 3
- 4
- 5

c

TRH:MDC1
AGT:NOS3
COL2A1:SMAD3
OSM:PLA2G2A
FGF10:ETS1
CCL2:LTB
CCL5:EGR1
CCL5:MMP9
COL1A1:ZFP36
MMP9:JUN
VWF:STAT5A
NTF4:GSN
APOE:CYP7B1
F8:CKS1B
NPNT:EPHA7
RPS19:VEGFA
VEGFB:MUC1
PSAP:AJUBA
CCL4:CBX4
COL1A1:IER3
FN1:ATF3
SAA1:ATF3
SEMA3C:NFE2L2
THBS1:ATF3
TNC:FOXO3
COL4A1:ID3
FBN1:DUSP1
FBN1:JUNB
FBN1:MYC
LAMC2:TCF4
NAMPT:CD36
POMC:FOS
TGFB1:COL5A1
TGFB1:MMP2
TGFB1:PDGFRB
TGFB1:FBN1
CCL14:GSN
C5:CXCR4
C5:PTMA
ANGPT1:ZFHX3
CXCL5:NR2F2
NTF3:TP53
IL10:KIF1BP
CXCL5:CCL2
TAC1:HMOX1

Communication sub-domains

ligand-target activity

1.0
0.8
0.6
0.4
0.2
0.0

d

Endothelial Lymphatic LYVE1
CAFs MSC iCAF-like
NK cells
T cells CD4+
B cells Memory
B Cells Naïve
T cells CD8+
NKT cells
Cycling T-cells
DCs
Endothelial CXCL12
PVL Differentiated
Endothelial ACKR1
Macrophage
Myoepithelial
Monocyte
Plasmablasts
Cycling Myeloid
PVL Immature
CAFs myCAF-like
Endothelial RGS5
Mature Luminal
Cancer Basal SC
Cancer Cycling
Luminal Progenitors

Cell type distribution

1.0
0.8
0.6
0.4
0.2
0.0

e

Celltype annotations

- Cancer Basal SC
- Cancer Cycling
- T cells CD4+
- CAFs myCAF-like
- T Cells CD8+
- PVL Differentiated
- CAFs MSC iCAF-like
- Luminal Progenitors
- Mature Luminal
- Myoepithelial
- Endothelial ACKR1
- Macrophage
- Plasmablasts
- Cycling Myeloid
- NK cells
- Cycling T-cells
- NKT-cells

Average neighborhood score

0   0.2   0.4   0.6   0.8   1.0

Ligand score

0   0.2   0.4   0.6   0.8   1.0

Supplementary Figure 7: (a) UMAP embeddings and (b) spatial map of communication sub-domains of domain 0 of the TNBC sample. (c) Differentially active ligand-target pairs across the communication sub-domains of domain 0. (d) Inferred cell type distribution across the communication sub-domains. (e) Ranking of ligands based on their cumulative activities over target genes expressed by major cell types in domain 0.
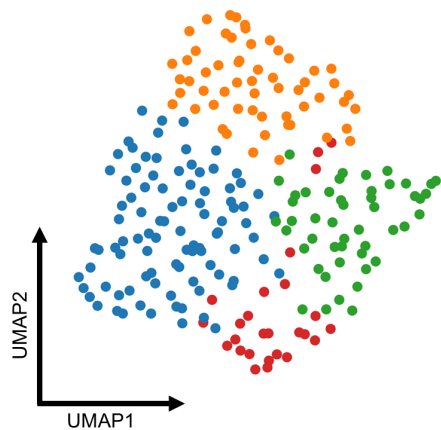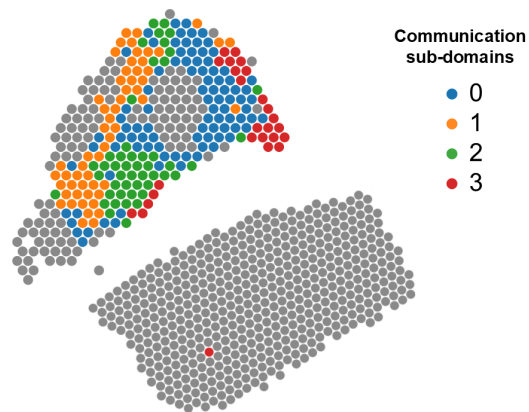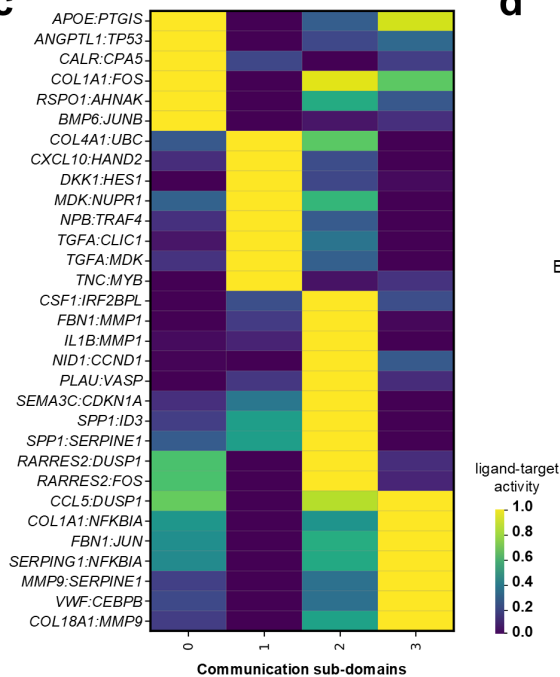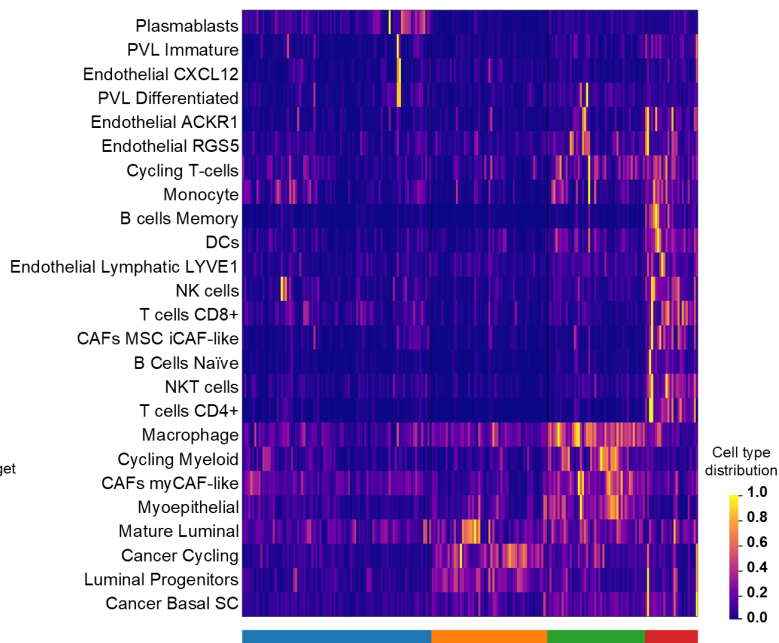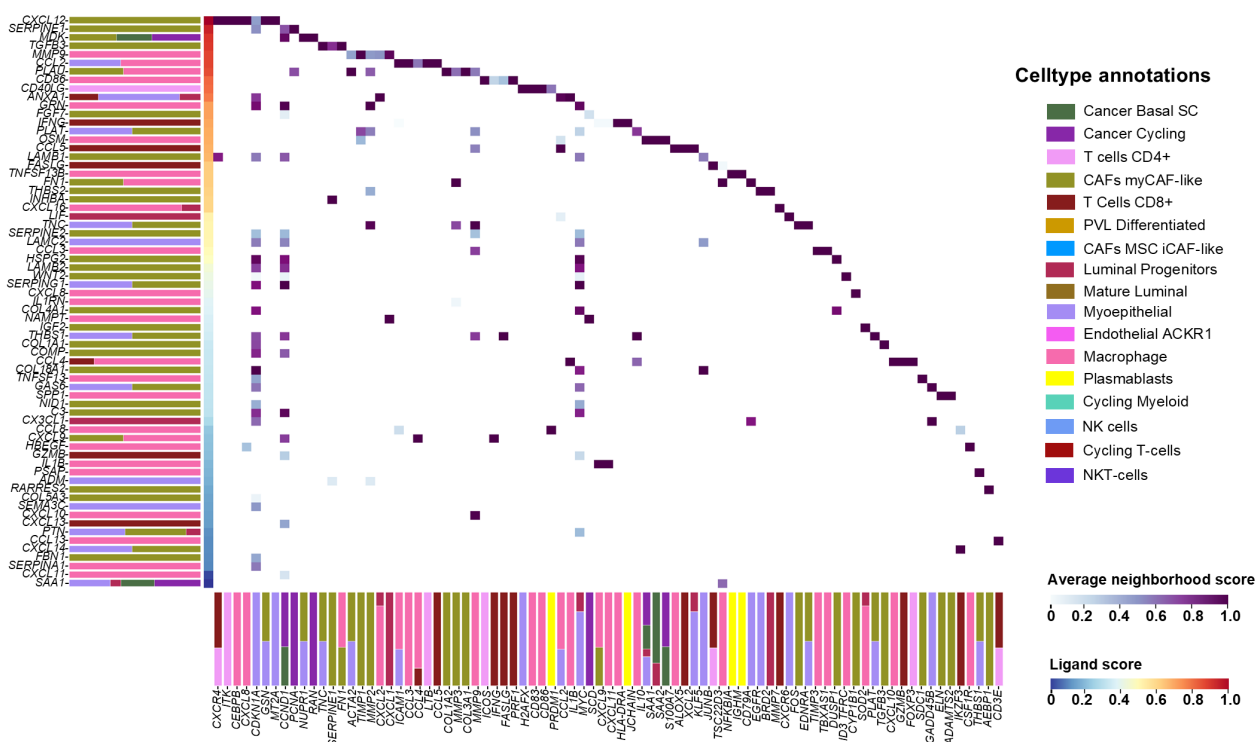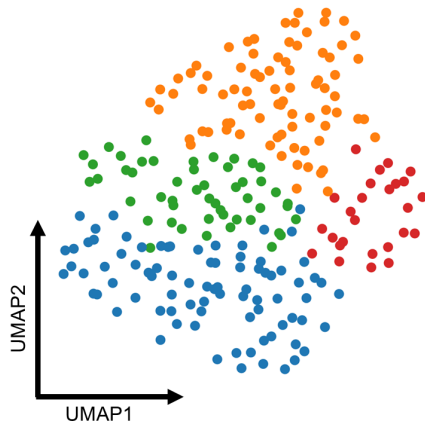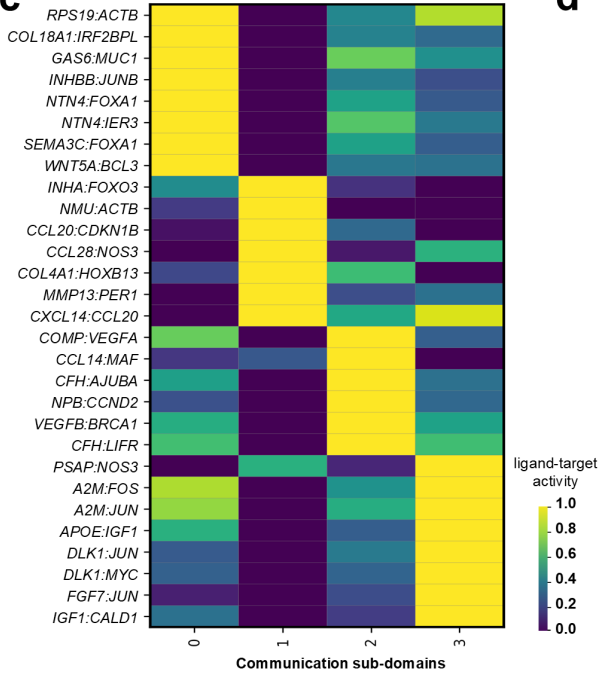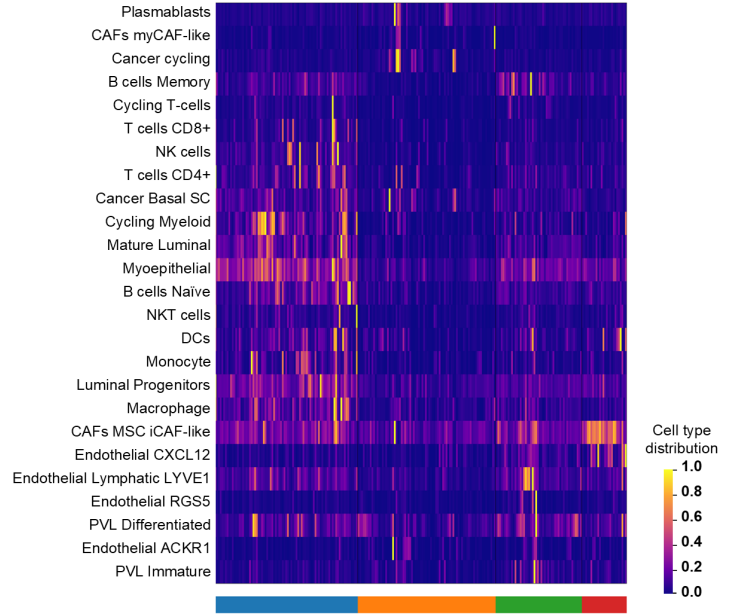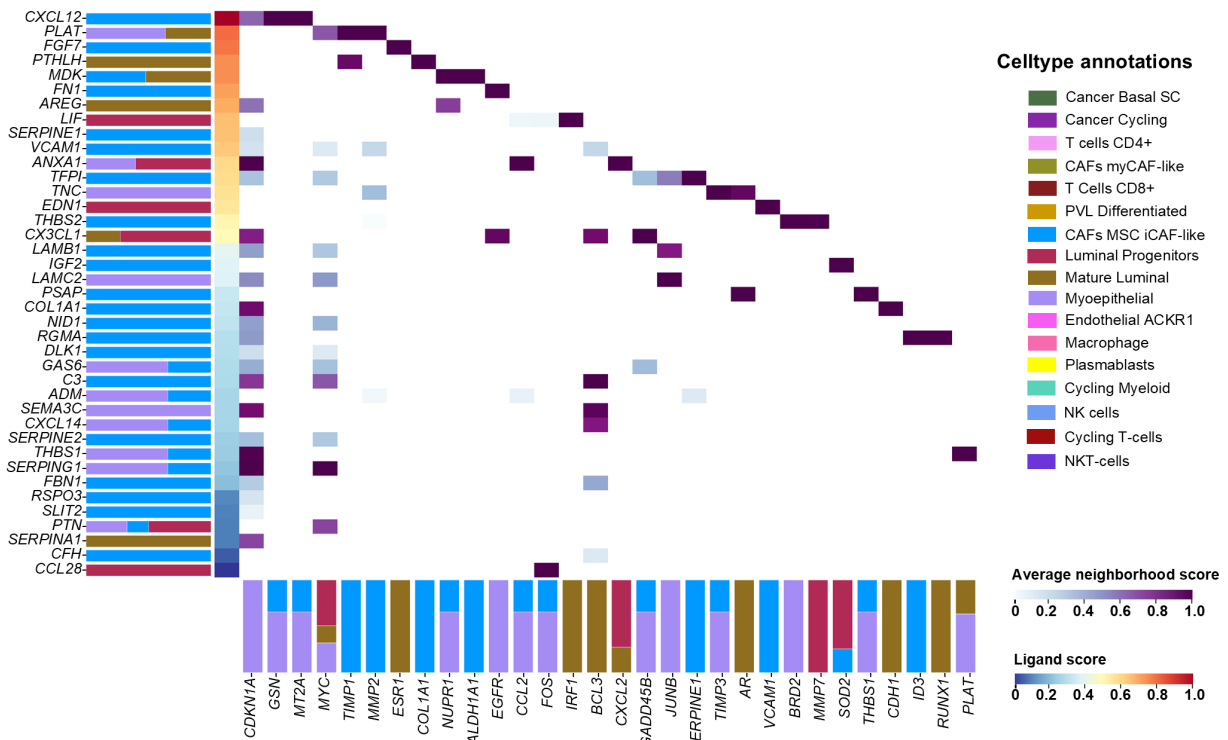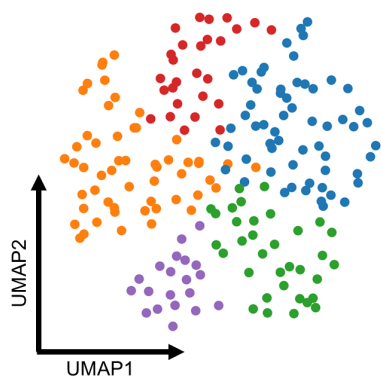
Supplementary Figure 8: (a) UMAP embeddings and (b) spatial map of communication sub-domains of domain 1 of the TNBC sample. (c) Differentially active ligand-target pairs across the communication sub-domains of domain 1. (d) Inferred cell type distribution across the communication sub-domains. (e) Ranking of ligands based on their cumulative activities over target genes expressed by major cell types in domain 1.
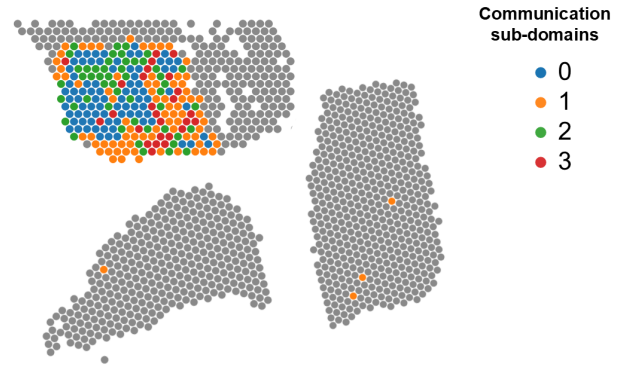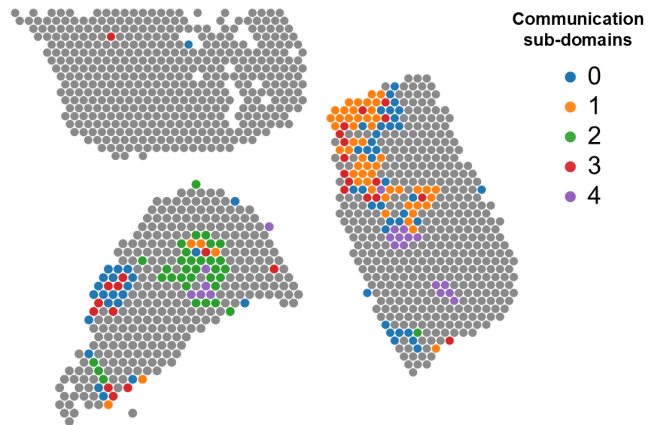
Supplementary Figure 9: (a) UMAP embeddings and (b) spatial map of communication sub-domains of domain 2 of the TNBC sample. (c) Differentially active ligand-target pairs across the communication sub-domains of domain 2. (d) Inferred cell type distribution across the communication sub-domains. (e) Ranking of ligands based on their cumulative activities over target genes expressed by major cell types in domain 2.
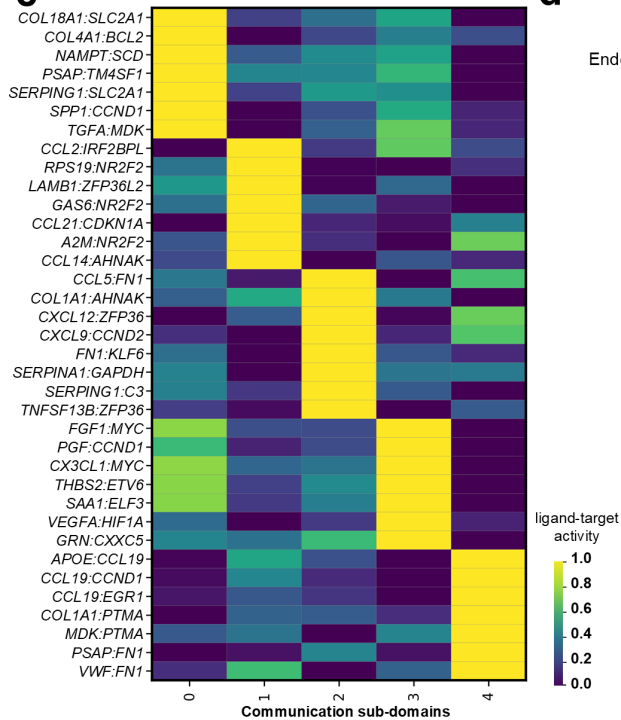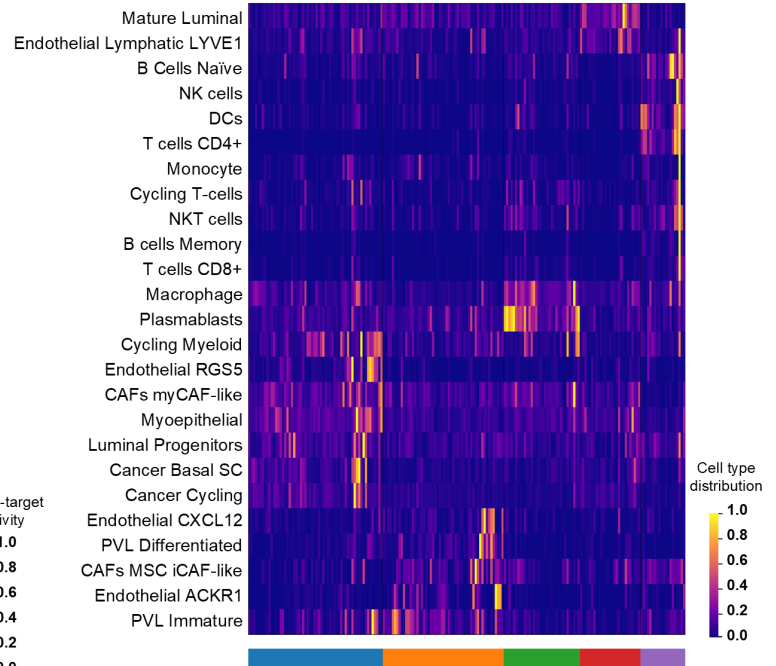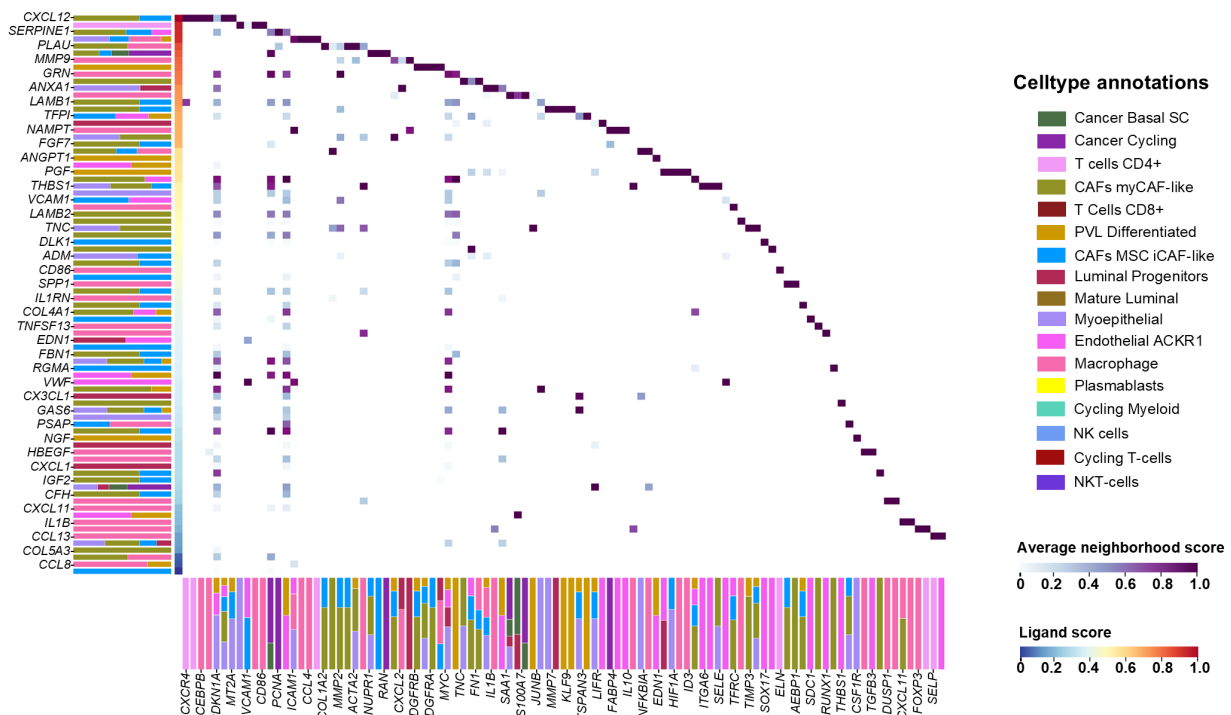
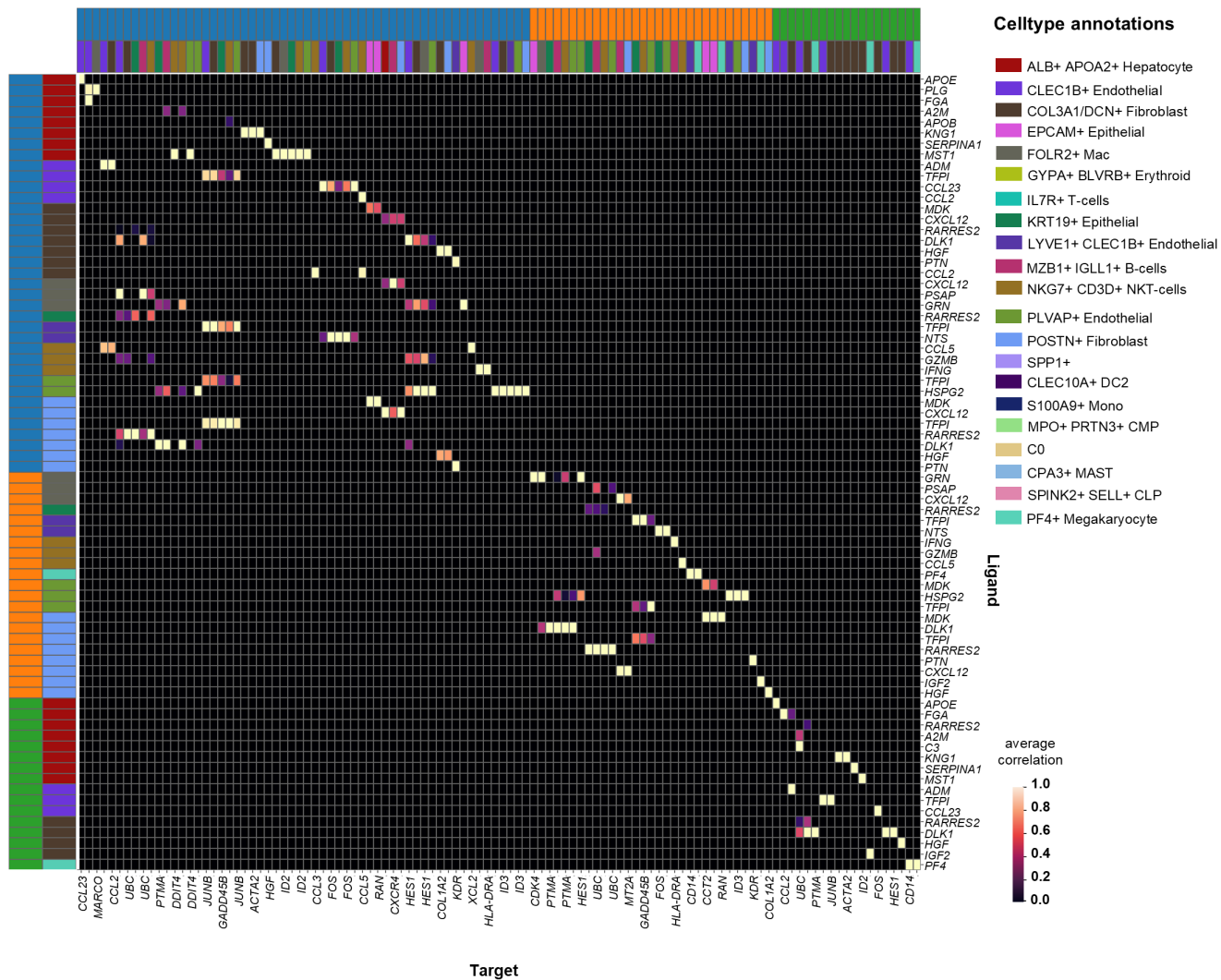Supplementary Figure 10: (a) UMAP embeddings and (b) spatial map of communication sub-domains of domain 3 of the TNBC sample. (c) Differentially active ligand-target pairs across the communication sub-domains of domain 3. (d) Inferred cell type distribution across the communication sub-domains. (e) Ranking of ligands based on their cumulative activities over target genes expressed by major cell types in domain 3.
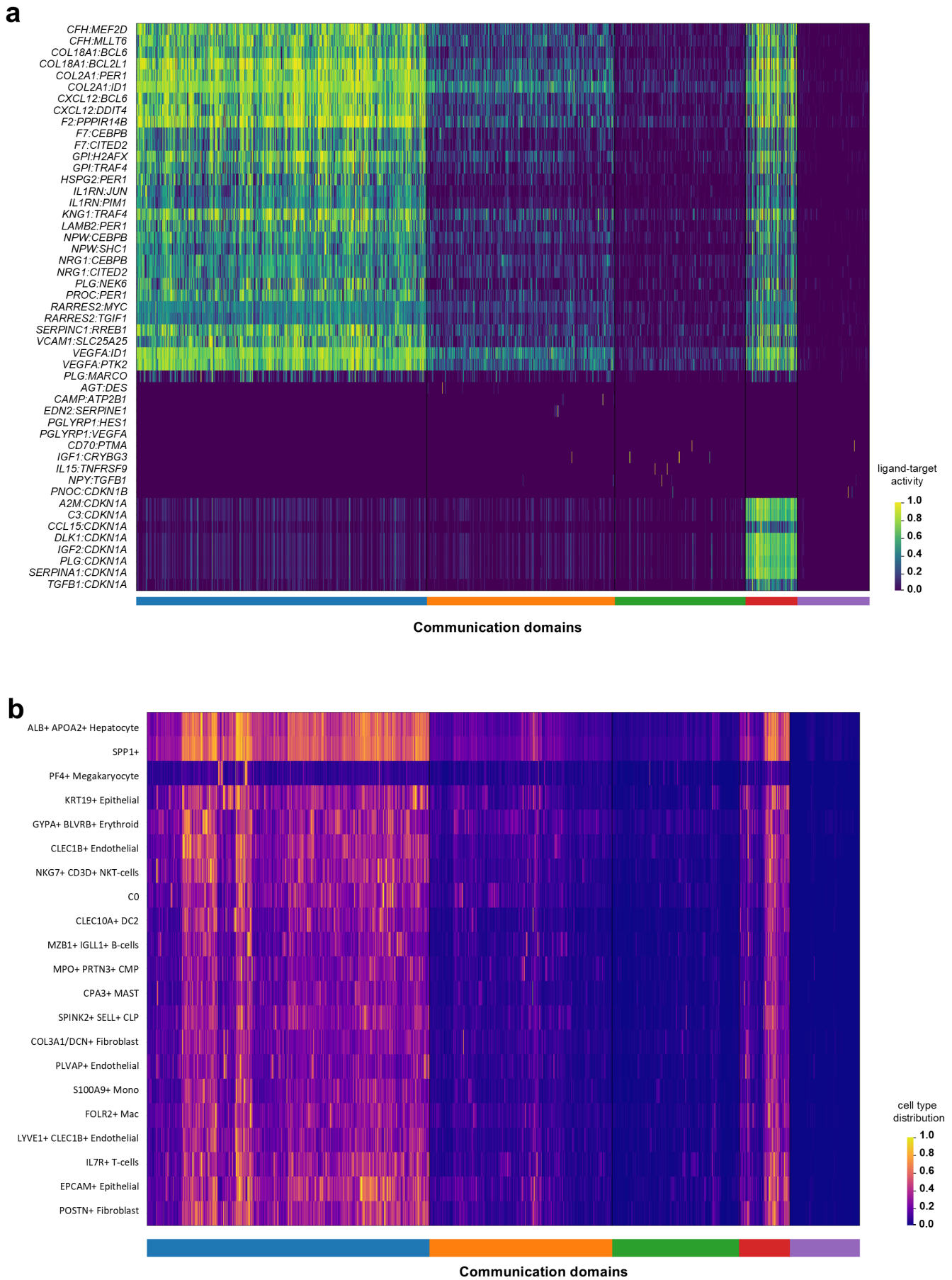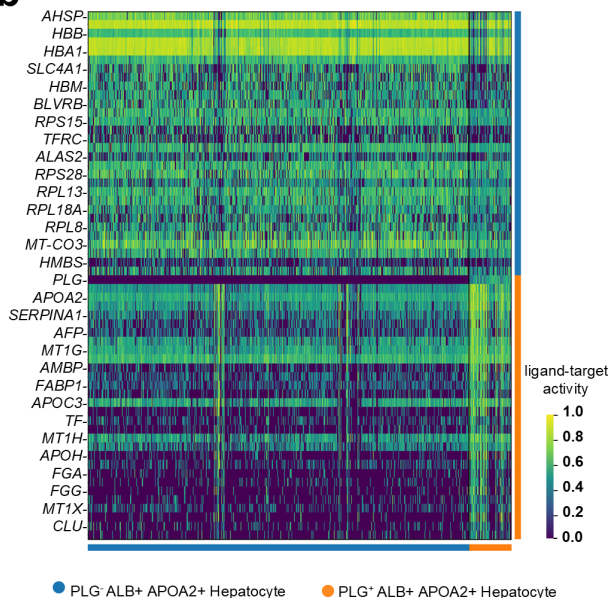
Supplementary Figure 11: (a) Differentially active ligand-target pairs inferred by Renoir across all communication domains for the fetal liver dataset. (b) Distribution of cell types across spots in the fetal liver dataset.

a

Celltype annotations

- ALB+ APOA2+ Hepatocyte
- CLEC1B+ Endothelial
- COL3A1/DCN+ Fibroblast
- EPCAM+ Epithelial
- FOLR2+ Mac
- GYPA+ BLVRB+ Erythroid
- IL7R+ T-cells
- KRT19+ Epithelial
- LYVE1+ CLEC1B+ Endothelial
- MZB1+ IGLL1+ B-cells
- NKG7+ CD3D+ NKT-cells
- PLVAP+ Endothelial
- POSTN+ Fibroblast
- SPP1+
- CLEC10A+ DC2
- S100A9+ Mono
- MPO+ PRTN3+ CMP
- C0
- CPA3+ MAST
- SPINK2+ SELL+ CLP
- PF4+ Megakaryocyte

b

- PLG⁻ ALB+ APOA2+ Hepatocyte
- PLG⁺ ALB+ APOA2+ Hepatocyte

Supplementary Figure 12: (a) Cell type-specific ligand-target interactions inferred by Renoir for the major cell types in domains 0, 1, and 2. The inner color bar represents the cell types of the ligand (left) and target (top) and the outer color bar represents the communication domain. Each cell represents the average Pearson correlation between the ligand-target neighborhood scores and the abundances of the cell types expressing the ligand and target across the spots pertaining to the domain being considered. (b) Differentially expressed genes between PLG^+ and PLG^- Hepatocyte populations.
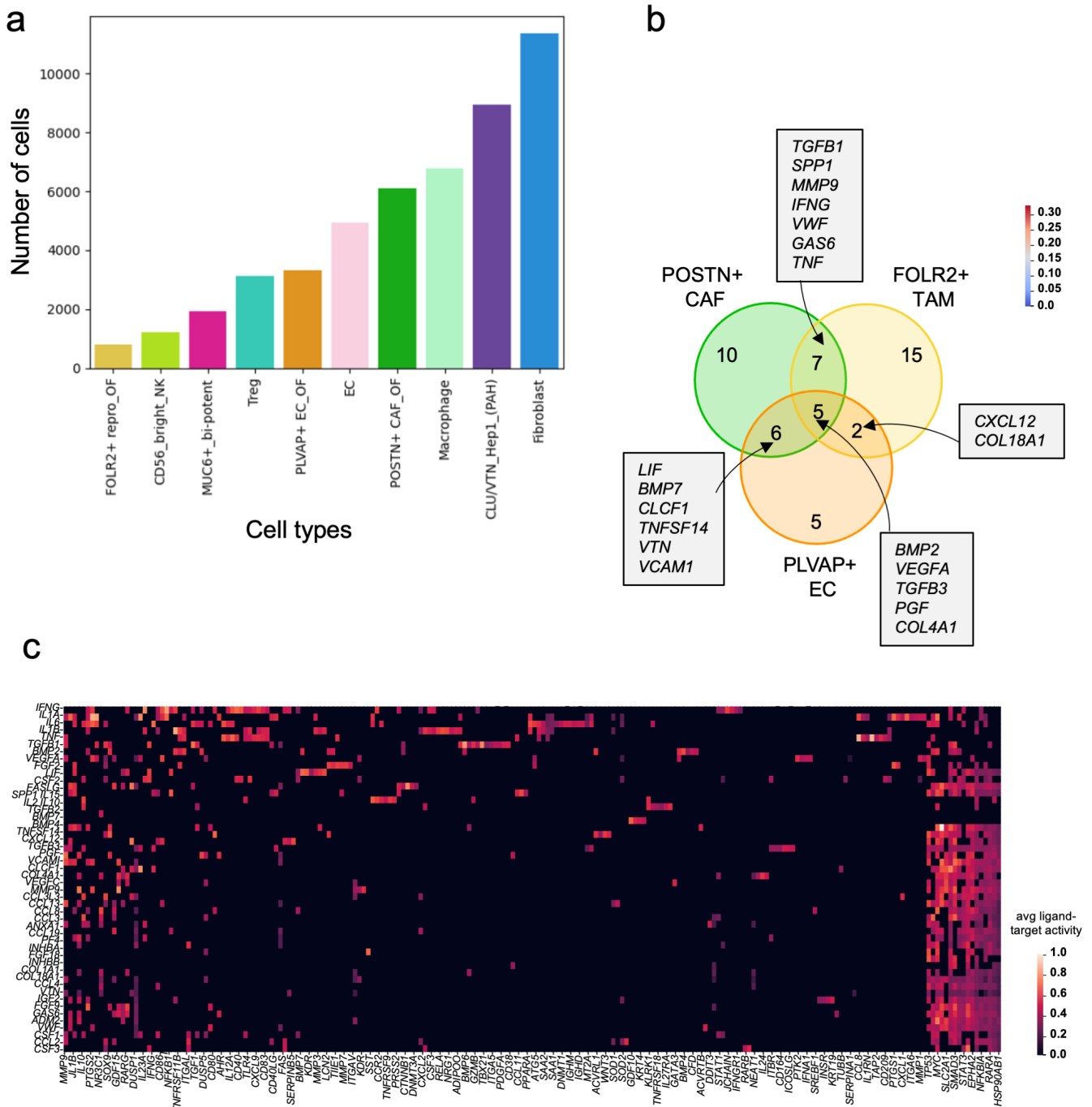
Supplementary Figure 13: (a) Distribution of major cell types located in the neighborhoods of onco-fetal cell types for the Nanostring CosMx hepatocellular carcinoma dataset. Cell types are ranked in the ascending order based on their number. (b) Venn diagram depicting the distribution of top 50 ranked ligands across onco-fetal cell types they are associated to. (b) Heatmap of cell type-specific activity ($MUC6^+$ bipotent cells) for ligand-target pairs with high average scores in the neighborhoods harboring onco-fetal cells and $MUC6^+$ bipotent cells.

Supplementary Tables

Supplementary Table 1: Association of genes in deferentially active ligand-target pairs and corresponding communication domains (inferred for mouse brain dataset) with known anatomical brain regions (with supporting literature).

Gene	Associated Communication Domain	Associated Region	Supporting Literature
Ccnd1	13	Amygdala	www.proteinatlas.org/ENSG00000110092-CCND1/brain
Nr2f2	13	Amygdala	www.proteinatlas.org/ENSG00000185551-NR2F2/brain
Cort	0	Cortex	www.proteinatlas.org/ENSG00000241563-CORT/brain
Rspo1	9	Cortex	www.proteinatlas.org/ENSG00000169218-RSPO1/brain
Vip	5	Cortex	elifesciences.org/articles/55130
Crlf1	16	Hippocampus	www.proteinatlas.org/ENSG00000006016-CRLF1/brain
Il16	17	Hippocampus	www.proteinatlas.org/ENSG00000172349-IL16/brain
Ntf3	16	Hippocampus	learnmem.cshlp.org/content/13/3/307
Dlk1	3	Hypothalamus	journals.plos.org/-plosone/article?id=10.1371/journal.pone.0036134
Tac1	14	Hypothalamus	academic.oup.com/endo/article/156/2/627/2422577
Tgfa	7	Striatum	www.jneurosci.org/content/8/6/1901.long
Avp	15	Thalamus	onlinelibrary.wiley.com/doi/10.1002/cne.22635
Lef1	2	Thalamus	link.springer.com/article/10.1007/s00429-012-0474-6
Ntng1	2,10	Thalamus	molecularbrain.biomedcentral.com/articles/10.1186/1756-6606-7-19
Tcf7l2	2,10	Thalamus	link.springer.com/article/10.1007/s00429-012-0474-6; neuraldevelopment.biomedcentral.com/articles/10.1186/s13064-018-0107-8
Cntn2	1	White Matter	www.proteinatlas.org/ENSG00000184144-CNTN2/brain; www.frontiersin.org/articles/10.3389/fncel.2019.00454/full
Csf1	1	White Matter	www.frontiersin.org/articles/10.3389/fimmu.2019.02199/full

Supplementary Table 2: Association of top-ranked ligands and corresponding communication domains (inferred for mouse brain dataset) with known anatomical brain regions (with supporting literature).

Gene	Associated Communication Domain	Associated Region	Supporting Literature
Bdnf	16	Hippocampus	https://www.nature.com/articles/4001957
Igf1	5	Cortex	www.frontiersin.org/journals/cellular-neuroscience/articles/10.3389/fncel.2017.00014/full
Vegfa	3	Thalamus	link.springer.com/article/10.1007/s00018-013-1280-x
Nrg1	1	Cortex	www.sciencedirect.com/science/article/pii/S221112471400610X
Npy	0	Amygdala	www.nature.com/articles/s41467-024-49766-0
Nrg2	5	Cortex	https://www.nature.com/articles/mp201722